Research Square

Preprints are preliminary reports that have not undergone peer review.
They should not be considered conclusive, used to inform clinical practice,
or referenced by the media as validated information.

Impact of Repeated Temperature Cycling on the Low-Concentration CO2 Adsorption Capacity of Grafted Silica-Amine †

Charlotte Wentz

cwentz@coastal.edu

National Institute of Standards and Technology

Sean McGivern

National Institute of Standards and Technology

Maxwell Mevorah

National Institute of Standards and Technology

Zois Tsinas

National Institute of Standards and Technology

Jeffrey Manion

National Institute of Standards and Technology

Amanda Forster

National Institute of Standards and Technology

Research Article

Keywords:

Posted Date: June 29th, 2026

DOI: https://doi.org/10.21203/rs.3.rs-9544331/v1

License: This work is licensed under a Creative Commons Attribution 4.0 International License.
Read Full License

Additional Declarations: No competing interests reported.

Abstract

The use of short-chain ethyleneimines (SCEI) and polyethyleneimines (PEI) as CO_2 sorbents has been extensively studied as a potential means of capturing carbon dioxide directly from the atmosphere. Previous work on such sorbents has focused on concentrated sources of CO_2, such as found in combustion exhaust streams, as well as 400 μLL − 1 CO_2 concentrations more typical of the atmosphere. In this study, we examine changes in the adsorption properties and physical, chemical, and morphological changes induced in grafted SCEI, specifically diethyleneimine and triethyleneimine chains grafted onto two high surface- area silica supports, MCM-41 and SBA-15, when subjected to large numbers of thermal cycles in dry, CO_2-free air. Emphasis is placed on the adsorption at 400 μLL − 1 CO_2 at 25 ∘C to study the potential suitability of similar grafted imine-containing systems for use as direct air capture (DAC) sorbents. For comparison, we also examine changes in the adsorption capacity at CO_2 concentrations of 5%, which are more typical of combustion exhaust. Notably, the low-concentration capacity is found to generally decrease faster than the capacity at the higher concentration with increased thermal cycling. All sorbents were found to decrease in adsorption capacity after a large number of cycles; however, DAS-derived sorbents were in general more robust. Moreover, the decrease in the CO_2 adsorption capacity at 25 ∘C before and after thermal cycling was found to vary significantly with the adsorptive concentration.

1 Introduction

A potential avenue for mitigating anthropogenic global warming is the capture of CO_2 from the exhaust streams of fixed combustion systems and directly from the atmosphere, the latter process known as direct air capture (DAC). DAC is particularly crucial in reaching net-zero carbon emissions in an environment where some fossil fuel combustion remains necessary to ensure safety and quality-of-life.[1] One heavily studied approach to DAC is the use of solid sorbents to reversibly adsorb ambient CO_2. Such sorbents allow capture and subsequent transport to a different location for CO_2 storage, typically in underground reservoirs, or use as industrial feedstocks. Unfortunately, existing solid sorbents show poor adsorption capacity, in moles of CO_2 per kilogram of sorbent (or $mmolg^{-1}$), at the low atmospheric concentrations of CO_2 (approximately 400 μLL^{-1}) as compared to much higher concentrations (100 to 300 times higher) found in combustion exhaust.[2–6] Recent efforts have focused on finding CO_2 sorbents that have both high capacities at atmospheric concentrations and are robust to repeated regeneration cycles, which for many solid sorbents occurs via heating for CO_2 removal and reactivation to enable additional adsorption after cooling.

In this study, we apply a range of both commercial and NIST constructed analytical techniques to study the low-concentration CO_2 adsorption performance of diamino- and triamino- short chain ethyleneimines (SCEI) grafted to two well-understood mesoporous silica substrates, SBA-15 and MCM-41*. Specifically, dynamic column breakthrough (DCB) measurements with an in-house constructed system[7] are used to

investigate adsorption capacity of CO_2 at concentrations of 400 μLL^{-1}. Additionally, we employ thermal gravimetric analysis (TGA) to study amine/organic loading, Fourier-transform infrared spectroscopy (FTIR) for surface chemistry, and scanning electron microscopy (SEM) to examine morphology. Central to this study, we probe the effects of temperature cycling in the absence of the adsorptive on sorbent adsorption properties by examining freshly synthesized materials and then subjecting samples to up to 300 controlled thermal regeneration cycles by alternately purging with a flow of hot or cold dry CO_2-free air. Properties were redetermined at selected cycling intervals. In addition, to understand how cycling behavior in an oxidative environment might be affected by CO_2 concentration, separate TGA experiments were conducted on samples exposed to CO_2 concentrations of 5% by volume (consistent with flue gas concentrations) for comparison with those taken at DAC-relevant concentrations.

2 Experiment

2.1 Materials. The MCM-41 and SBA-15 mesoporous silicas were both purchased from ACS Material and were dried in a vacuum oven at 110 ∘C for 2 h before use. Anhydrous toluene (99.8%, Aldrich) was used without further purification. *N*- [3-(trimethoxysilyl)propyl] ethylenediamine (DAS), and *N*1- (3-trimethyoxysilylpropyl) diethylenetriamine (TAS) were purchased from Sigma-Aldrich and used without further purification. Carbon dioxide (ULSI grade, 99.999%, Matheson) and nitrogen (ultrahigh purity, 99.999%, Roberts Oxygen) were used in the DCB and TGA experiments. The air utilized for the cycling experiments was purified and dried through a Parker-Balston FT-IR Purge Gas Generator (< 1 μLL^{-1} CO_2, dew point < − 73 ∘C).

2.1.1 Synthesis. The sorbent samples examined in this work are short-chain ethylene imines (SCEI) covalently grafted to mesoporous silica substrates (Fig. 1). To synthesize these samples, dry mesoporous silica support (MCM-41 or SBA-15) was placed in a Schlenk round bottom flask equipped with a polytetrafluoroethylene stir bar with 5 volume equivalents of anhydrous toluene (as noted by a reviewer, less toxic solvents[8] are likely acceptable). Similar to previous work,[9–11] deionized water (0.07mL/g silica) was added to expand the pores in the silica for increased amine loading, and the mixture was left to stir for approximately 10 min. The aminosilane was subsequently added to the flask at about 90% mass fraction (approximately 1.5 g silane/g silica). This reaction vessel was fitted with a condenser and heated to 100 ∘C for ≈ 6 h. The product mixture was allowed to cool to room temperature before being vacuum filtered and washed three times with copious amounts of toluene. Finally, the washed solid was dried in a vacuum oven at 100 ∘C for ≈ 18 h. The naming convention used in this work for the sorbent samples is the SCEI/aminosilane abbreviation followed by mesoporous silica substrate: DAS/SBA-15, TAS/SBA-15, DAS/MCM-41, and TAS/MCM-41. Note that the present synthesis procedure was optimized for simplicity and reproducibility and is not expected to produce the highest adsorption capacity. The amine content of the freshly synthesized samples was estimated using TGA and will be described below.

2.2 Analytical Procedures. An overview of the complete analytical procedure for each of the four samples is shown in Fig. 2. Samples were initially characterized after synthesis using TGA, FTIR, and SEM; detail on the individual analyses are provided below. Once characterization was complete, ≈ 80 mg samples were pressed into a 1 cm disc with a pellet press with a constant 6.7N force, ground lightly with a mortar and pestle, and sieved to a size range of (425 to 600) μm granules to facilitate additional studies, which require a packed bed capable of supporting flow. Samples were confirmed to have equal adsorption capacity at 5% CO_2 in N_2 before and after granularization to within reported uncertainties. All reported measurements after the initial characterization are on granular samples.

After granules were formed, an initial DCB analysis was performed to determine the equilibrium adsorption capacity when exposed to 400 μLL^{-1} CO_2 in He. Samples were then subjected to repeated temperature cycles in flowing dry air from approximately (30 to 80) ∘C over 5 min and back down to 30 ∘C over an additional 5 min. These 10 min heating-cooling cycles were repeated up to 300 times with periodic pauses for DCB analysis and removal of a small aliquot of the samples for other analyses. Cycling was terminated prior to 300 cycles in those cases where the capacity had been deemed to be substantially reduced. Exact cycle numbers are presented with the results for each sample.

2.2.1 Thermogravimetric Analysis of Amine Content. Thermogravimetric analysis (TGA) was used to estimate the amine content/organic loading of the grafted samples in lieu of elemental analysis which was not available for this study. Analysis was performed with a TA Instruments Discovery TGA 550 thermogravimetric analyzer, having respective mass and temperature uncertainties of $\pm$ 0.01% and $\pm$ 1 ∘C. Prior to analysis, samples were equilibrated at 30 ∘C for ≈5 min under high-purity N_2 flowing at $60 mL min^{-1}$. No mass loss was observed during equilibration. The analysis was performed by ramping the temperature at 10 ∘C/min to 1000 ∘C. Several fresh samples exhibited a rapid mass loss of ≈5% below 200 ∘C that is not evident in thermograms for cycled samples (see Figures S1 to S7 in supporting information†). We attribute low-temperature losses to adsorbed water, solvent, or gas from the synthesis, although we cannot rule out loss of high vapor pressure amines or other organic compounds. Fresh samples were analyzed three times to obtain the mass loss and associated uncertainty (see below in Table 3). Cycled materials were analyzed only once due to the destructive nature of TGA.

The TGA instrument used in the present amine-loading analysis is not capable of identifying specific decomposition products. However, in the fresh samples only solvent, amine, and small amount of water have contacted the thermally stable substrates. Therefore, excluding the low-temperature losses discussed above, it is reasonable to assume that weight losses at higher temperatures in uncycled samples are due to loss of amines. This assumption may be less valid for the cycled samples, which show evidence of chemical changes as will be evident below. In cycled samples, the TGA mass losses likely include both amines and reaction products arising from the uncertain chemical changes induced by thermal cycling. For brevity, we often refer to these losses as “amine losses” but note that this is strictly accurate only for the fresh samples. Note pure SBA-15 or MCM-41 show slight mass losses of (2

to 6) % over this temperature range (Figures S6 and S7 in supporting information†) that are not factored into the reported results or uncertainty.

2.2.2 Thermogravimetric Analysis of Adsorption Capacity. TGA was also used to measure CO_2 adsorption at higher CO_2 concentrations to provide a comparative adsorption capacity for non-DAC conditions, such as would be found in a combustion flue gas, and to evaluate if property changes caused by thermal cycling are similar in samples exposed to very different CO_2 concentrations. In these TGA studies, samples were first activated at 100 ∘C for 5 min under flowing N_2 before cooling to 40 ∘C at rate of 10 ∘C/min. The material was then held at 40 ∘C for 5 min before introducing a mixture of 5% CO_2 in N_2 for 30 min. The heating and cooling steps were repeated times to obtain three adsorption/desorption curves for each sample. The observed weight gain during the experiment is attributed to the total uptake of CO_2 with the capacity of N_2 assumed to be negligible since pure N_2 studies have shown no significant uptake. Thermograms are available in the supporting information† for each material (Figures S8 to S11). For all samples, the capacity loss was measured before and after a long (> 1500 min) heating under a 50 $cm^3 min^{-1}$ flow of dry CO_2-free air at 80 ∘C and minimal variations (< 6%, Table S3) were observed. Since this length of time exceeded the total time samples were subjected to high temperatures from the thermal cycling described below, the changes noted in this work are attributed primarily to the cycling itself and are not expected to be derived solely from heating.

2.2.3 Dynamic Column Breakthrough. Dynamic column breakthrough (DCB) experiments were used to determine equilibrium adsorption capacities at 400 μLL − 1 on a NIST-constructed apparatus described in detail previously.[7]

Briefly, ≈ 200 mg of granular material is placed into a 6mm diameter column and activated with a 500 $cm^3\ min^{-1}$ purge flow of He at 80 ∘C for 1 h. To initiate the experiment, a rotary valve is used to expose the column to a 500 $cm^3\ min^{-1}$ flow of 400 μLL^{-1} CO_2 in He using a pair of mass-flow controllers while monitoring the outlet concentration for 2000 s using a mass spectrometer fixed at 44 Da. Outlet CO_2 concentrations are initially zero as the material fully adsorbs the CO_2 but increase over time until saturation is reached, where the observed outlet concentration is the same as the inlet concentration. The total area of the adsorbed 44 Da mass spectrometer signal can be compared to the known input molar flow rate to determine the amount of CO_2 adsorbed by the known mass of material. The NIST DCB apparatus has been shown to accurately (within 0.05 $mmol g^{-1}$) measure CO_2 adsorption capacities even at low CO_2 concentrations (400 μLL^{-1}) that mimic DAC conditions.[7]

2.2.4 Temperature Cycling Apparatus and Procedure. Following an initial capacity measurement, the column containing the sample under study was removed from the DCB apparatus and immediately inserted into the temperature cycling apparatus, which uses identical attachment fittings. Temperature cycling of the material was then accomplished by repeatedly switching a flow of heated or room-temperature dry and CO_2-free air through the material. A schematic of the apparatus is provided in Fig. 3,

which shows flow paths during the heating (a) and cooling (b) phases of each temperature cycle. During the heating phase of a given cycle, ambient temperature purge air was heated by directing it through a coiled copper line in an oven, after which the gas was passed through the column containing the sorbent for a fixed time (300 s in the present study). The cooling phase for the temperature cycle was then initiated by switching a rotary valve to redirect the air flow and bypass the oven, thus passing room temperature air through the column. Additionally, at the beginning of each cooling phase, an external fan directed at the cell was switched on with a computer-controlled relay to aid cooling, Fig. 3.

At fixed intervals during the cycling (after 15, 100 and 200 cycles for TAS and 100, 200 and 300 cycles for DAS), the material column was removed from the temperature cycling system and transferred to the DCB apparatus for capacity measurements, after which the column was reinstalled for further temperature cycling of the material. A small aliquot of material was removed for additional analysis prior to temperature cycling. The change in mass of the specimen is measured and taken into consideration for future DCB

capacity measurements. Breakthrough curves for all samples may be found in Figures S13 to S16 in supporting information†.

2.2.5 Fourier Transform Infrared Spectroscopy Measurements (FTIR). Fourier Transform infrared spectra of the samples were taken with a Nicolet iS50 FTIR spectrometer using a built-in attenuated total reflectance (ATR) cell and analyzed with the Nicolet OMNIC software included with the instrument. Each spectrum was collected using 128 scans with resolution of 4 cm^{-1}. Standard uncertainties associated with this measurement are $\pm$ 1% in peak intensity and $\pm$ 4 cm−1 in wavenumber. The instrument software's ATR baseline correction is applied to all spectra.

2.2.6 Scanning Electron Microscopy (SEM). Materials in powder form were carefully spread on aluminum stubs under a stereo microscope and fixed using carbon conductive dual-sided tape. Each material was sputter coated with about 5 nm-thick Au–Pd conductive coating for optimal imaging conditions. Samples of the pure silica substrates and fresh grafted materials, as well as crushed materials taken from the thermally cycled sample aliquots were imaged on a FEI Helios NanoLab 650 dual-beam SEM to probe sample morphology. The micrographs were collected under high vacuum (i.e., less than 0.4 mPa [3×10^{-6} Torr]), at a beam energy of 2 keV and probe current of 25 pA. Scan parameters were optimized to minimize charging, artifacts, and drift.

3 Results and Discussion

The present study utilizes well-known and readily synthesized materials to focus on a novel testing procedure wherein we repeatedly pass heated zero-air (i.e. CO_2- and H_2O-free) through the sample to subject the material to numerous temperature cycles. Specifically, DAS/SBA-15 and DAS/MCM-41 samples were collected at 100, 200 and 300 temperature cycles, and TAS/SBA-15 and TAS/MCM-41 samples were collected at 15, 100 and 200 cycles. Initial experiments showed the TAS-containing

samples to be broadly less robust with respect to temperature cycling in an oxidative environment, so experiments were redone with an additional early-run analysis and stopping the temperature cycling after 200 for those samples. As noted above, at each point, TGA (both amine loading and high-concentration CO_2 capacity), DCB, FTIR, and SEM analyses were performed, and results from these analyses will be discussed in terms of adsorption capacity, chemistry, and physical and morphological changes. In addition, porosity studies for the two substrates have been reported previously.[12]

3.1 Adsorption Capacity. Adsorption capacities from DCB measurements at 400 μLL^{-1} CO_2 in He are provided for all samples in Table 1. Typical DCB curves are shown in Fig. 4 and Figures S14 to S16 in supporting information†. The shaded regions in the figures represent CO_2 adsorbed by the sorbents and visually indicate changes in the adsorption capacity. As noted above when discussing the synthesis of the samples, a primary goal of this study is to examine how these SCEI compounds behave at concentrations consistent with DAC rather than developing a new DAC material. All of these samples show low adsorption capacity and would themselves be unsuitable as functional DAC sorbents even fresh. For both amines, the SBA-15 based substrates showed higher capacity even when fresh than the MCM-41 substrates, particularly in the case of TAS, despite the MCM-41 having a larger manufacturer specified surface area ((900 to 1100) $m^2\ g^{-1}$ compared to (450 to 550) $m^2\ g^{-1}$ for SBA-15).

Table 1 Adsorbent capacities from DCB analysis of 400 μLL−1 CO2 in He of amine-grafted silica composites during thermal cycling.

Material	Thermal Cycles				
mmol g^{-1}	0	15	100	200	300
DAS/SBA-15	0.33	-	0.33	0.32	0.23
TAS/SBA-15	0.53	0.55	0.18	0.08	-
DAS/MCM-41	0.29	-	0.24	0.09	0.03
TAS/MCM-41	0.13	0.10	0.07	-	-

Thermal cycling in dry air causes an overall decrease in capacity for all samples. The TAS samples generally show a faster decrease in capacity with increasing cycle numbers compared to DAS, which is why the former were initially sampled at only 15 cycles. In three samples, small reductions in capacity were observed between the uncycled and initial cycled samplings (15 cycles with TAS/MCM-41 and 100 cycles with TAS/SBA-15) with more substantial decreases found with increased cycling in all cases. For the TAS/SBA-15, a 4% increase in capacity was found after 15 cycles; this is within the experimental uncertainty and is likely indicative of no change, consistent with the DAS/SBA-15 sample.

In general the amine-grafted SBA-15 samples were much more robust than the MCM-41 samples, showing no decrease between the first and second samplings for either amine. However, the TAS/SBA-15 TAS showed a rapid decrease at 100 cycles and was nearly deactivated as a sorbent by 200 cycles. The DAS/SBA-15 sample was quite robust, surviving 200 cycles with no significant decrease in capacity

before dropping 30% after 300 cycles. DAS was much less robust on MCM-41, maintaining most of its capacity after 100 cycles but having lost 61% capacity at 200 cycles and becoming nearly completely deactivated at 300 cycles. The measured capacity of even fresh TAS/MCM-41 is low, near the detection limit of the DCB instrument, and although we can discern a significant decrease after 100 cycles, no further quantitative conclusions can be drawn.

To facilitate comparison of these results with studies done at higher concentrations, TGA measurements of adsorption capacity of 5% CO_2 in N_2 were also performed and are presented in Table 2. As expected, the capacities measured at the higher CO_2 concentration are all higher than those at 400 μLL^{-1}. However, the large decrease between the fresh samples and the first sampled cycles (i.e. 15 for MCM-41 and 100 for SBA-15) is noteworthy. It appears that the fresh samples have moieties that react with CO_2 that are very unstable with respect to oxidation or heating. This large difference is

not seen in the 400 μLL^{-1} samples; it is unclear if this is a concentration effect or some effect of handling as samples were moved between instruments.

Otherwise, broad trends are similar with a few caveats. The large decrease after 300 cycles in DAS/SBA-15 to an absolute capacity lower than that measured at 400 μLL^{-1} is an anomaly, the origin of which is unclear. The DAS/MCM-41 sample maintains its capacity at higher concentrations when the 400 μLL^{-1} capacity shows a marked decrease between 200 to 300 cycles.

3.2 Chemistry. Amine loadings, or more generally amine and degradation product loadings derived from mass losses in TGA temperature-ramp experiments, are provided in Table 3. The loadings of the fresh materials broadly correlate to the high-concentration adsorption capacities but do not reflect the adsorption capacities at 400 μLL^{-1} in any apparent way. The change in the loadings does more closely reflect the capacities for the relatively robust DAS samples, although both samples exhibit mass increases after 100 cycles. The TAS samples show different trends depending on the substrate. The TAS/SBA-15 shows an early decrease and then a marked increase after 100 cycles and a slight decrease at 200 cycles where it is deactivated at both concentrations. The TAS/MCM-41 stays essentially constant at 15 cycles and then decreases. Given the extremely low adsorption capacity of this sample, particularly at 400 μLL^{-1}, and obviously low stability with respect to thermal cycling, we hypothesize that the behavior may be similar for both samples but the TAS/MCM-41 deactivates so quickly we were unable to observe the initial decrease followed by an increase during the 15-cycle interval. Due to the very low capacity at low concentrations, we did not attempt to explore this possibility further.

SCEIs, such as DAS and TAS, and polyethyleneimines (PEI) on silica substrates, both impregnated and covalently grafted as in the present work, have been the subjects of numerous previous CO_2 adsorption studies. In broad terms as discussed below, impregnated SCEI and PEI materials show higher capacity per amine than covalently grafted materials but are generally less robust to temperature cycling and can

slough off a substrate during regeneration. For comparison in the present work, we focus on previous studies at low CO_2 concentrations of impregnated and grafted materials.[13]

Table 2. Adsorbent capacities from TGA of 5% CO_2 in N_2 of amine-grafted silica composites during thermal cycling; samples with measured uncertainty have a n = 3.

Material	Thermal Cycles				
mmol g^{-1}	0	15	100	200	300
DAS/SBA-15	0.869 ± 0.037	-	0.406	0.374	0.073
TAS/SBA-15	0.858 ± 0.014	0.403	0.409	0.154	-
DAS/MCM-41	0.631 ± 0.013	-	0.486	0.462	0.436
TAS/MCM-41	0.720 ± 0.034	0.266	0.209	-	-

Table 3. Mass losses measured with TGA/temperature ramping (expressed in percent mass loss in each temperature cycle) in amine-grafted silica composites. As discussed in the text, fresh losses are assumed to be amine; mass losses from cycled samples may include other reaction products.

Material	Thermal Cycles					
	0	0	15	100	200	300
	mmol N/g[a]	%	%	%	%	%
DAS/SBA-15	1.14 ± 0.05	20.81	-	21.36	20.63	12.23
TAS/SBA-15	0.960 ± 0.016	25.60	22.11	34.93	31.20	-
DAS/MCM-41	0.699 ± 0.014	15.94	-	16.97	15.30	15.30
TAS/MCM-41	1.43 ± 0.03	28.44	28.24	14.24	-	-

[a]Moles of parent DAS or TAS lost in zero-cycle TGA run per gram of grafted sorbent

FTIR spectroscopy was also used to explore the chemical changes induced by the rapid temperature cycling. In general, spectra appear to be consistent with the extensive previous infrared spectroscopy done on SCEI and PEI samples, both grafted and impregnated.[9,14–16] The hydrocarbon regions > 2750 cm^{-1} show little change with increased cycling other than an overall decrease in magnitude. The present analysis focuses in the (1250 to 1850) cm^{-1} range, shown in Fig. 5 with full spectra provided as supporting information† (Figures S17 to S20). In particular, we note the growth of a peakaround 1670 cm^{-1} corresponding to either imine C =N formation within the ethyleneimine chain or C =O corresponding to formation of urea across chains. Other peaks appear to generally decrease with increased thermal cycling, a change presumed to be due to simple loss of material, which is also evident in the TGA thermal cycling experiments discussed previously.

In the DAS/MCM-41 spectra, peaks are generally small, likely a result of the poor amine loading on the samples compared to TAS samples. For the other samples, the 1670 cm^{-1} peak is qualitatively much larger relative to the peaks in this region for the SBA-15 samples compared to the TAS/MCM-41. As noted above, both SBA-15 samples show higher initial loading despite having a lower surface area, which would tend to favor cross-chain chemistry and urea formation and would be consistent with several previous NMR studies [17–19] that show strong evidence of C =O formation under oxidative thermal

degradation. More explicitly, both Pang, et al. and Li, et al. reported a correlation between the efficiency and stability of poly(propyleneimine)s (PPI) compared to PEI, regardless of secondary amine content.[20,21] Such stability was hypothesized to be due to greater spacing between chains in the PPI, which would inhibit deactivation due to urea formation. Furthermore, Builes and Vega calculated that binding of CO_2 by primary amines in ethyleneimines is enhanced when the chains are free to move closer to the substrate surface.[13] In the present, we can speculate that the binding at 400 $\mu L L^{-1}$ is especially facile prior to cycling when the grafted chains are most mobile and there is no cross-linking in the chains. In DAS and particularly TAS due to the additional secondary amine, cross-linking upon thermal cycling may lead to a notable drop at low CO2 concentrations due to decreased primary amine mobility but still allow significant binding at higher CO_2 concentrations via the less mobile but still available primary amines.

In broad terms, the presence of significant changes under cycling conditions that are not observed from simple heating may be due in part to oxidative processes. Cycling experiments are done in CO_2-free dry air, allowing oxygen to adsorb during the cold region of the temperature profile. Heating in the second half of the temperature cycling may then result in oxidative processes that occur repeatedly due to cycling but do not proceed in experiments in which samples were heated for a similarly long time but without exposure to cold air. The color changes discussed below are also consistent with such an interpretation, but additional studies are necessary to more solidly confirm deactivation of the sample via such pathways.

In the DAS/MCM-41 spectra, peaks are generally small, likely a result of the poor amine loading on the samples compared to TAS samples. For the other samples, the 1670 cm^{-1} peak is qualitatively much larger relative to the peaks in this region for the SBA-15 samples compared to the TAS/MCM-41. As noted above, both SBA-15 samples show higher initial loading despite having a lower surface area, which would tend to favor cross-chain chemistry and urea formation and would be consistent with several previous NMR studies[17–19] that show strong evidence of formation under oxidative thermal degradation. More explicitly, both Pang, et al. and Li, et al. reported a correlation between the efficiency and stability of poly(propyleneimine)s (PPI) compared to PEI, regardless of secondary amine content.[20,21] Such stability was hypothesized to be due to greater spacing between chains in the PPI, which would inhibit deactivation due to urea formation. Furthermore, Builes and Vega calculated that binding of CO_2 by primary amines in ethyleneimines is enhanced when the chains are free to move closer to the substrate surface.[13] In the present case, we can speculate that the binding at 400 $\mu L L^{-1}$ is especially facile prior to cycling when the grafted chains are most mobile and there is no cross-linking in the chains. In DAS and particularly TAS due to the additional secondary amine, cross-linking upon thermal cycling may lead to a notable drop at low CO_2 concentrations due to decreased primary amine mobility but still allow significant binding at higher CO_2 concentrations via the less mobile but still available primary amines.

In broad terms, the presence of significant changes under cycling conditions that are not observed from simple heating may be due in part to oxidative processes. Cycling experiments are done in CO_2-free dry

air, allowing oxygen to adsorb during the cold region of the temperature profile. Heating in the second half of the temperature cycling may then result in oxidative processes that occur repeatedly due to cycling but do not proceed in experiments in which samples were heated for a similarly long time but without exposure to cold air. The color changes discussed below are also consistent with such an interpretation, but additional studies are necessary to more solidly confirm deactivation of the sample via such pathways.

3.3 Physical and Morphological Changes. To further investigate potential changes in surface morphology induced by grafting, thermal cycling, and the underlying silica support itself, representative SEM images were taken and are presented in Fig. 6. As expected, these images reveal distinctly different morphologies for SBA-15 (6a), and MCM-41 (6b). The SBA-15 exhibits rod-shaped macroscale structures with diameters from ((10 to 100) μm) that are composed of smaller nanorod particles with less variability in diameter (≈ 200 nm) and in length (≈ 800 nm). On the other hand, MCM-41 (6b) shows clusters in the macroscale with diameters from (1 to 10) μm) with a 3D flower like nanoscale morphology on the surface. The grafted materials, prior to forming granules, show a slight change in topology, shown in Figs. 6c and 6d. Aged materials showed signs of more significant loss of the original structure, primarily due to the granularization of the materials required for the CO_2 adsorption capacity experiments (Figs. 6e and 6f). However, the presence of the original morphology of the neat materials in the nanoscale can still be distinguished in some areas of the materials, as highlighted by the red circles in Figs. 6e and 6f. Given the small decrease in capacity in the samples with low numbers of thermal cycles, it is likely that the granularization had little effect on the available surface area for adsorption of CO_2.

Simple visual observation over the course of the thermal cycling showed that the sample color darkened from white to a moderate yellow. Figure 7 shows images of the samples, which show a substantial color change upon increased thermal cycling. Note that the zero-cycle image in this figure is the powder form; others show the granular samples that have been pressed, crushed, and sieved to facilitate the DCB measurements and temperature cycling (see above). studies have noted color changes in SCEI and PEI samples upon exposure to elevated temperatures in the presence of O_2.[9,14,22] Srikanth and Chuang[15] studied the pentaamine analogous to DAS and TAS impregnated on silica samples at 100 ∘C for 12 h and noted an “intense yellow.” Those authors attributed the yellow color to imides formed via oxidation of the C–H bonds in the polymer chain based on FTIR and ^{13}C-NMR. The present FTIR spectra are consistent with this analysis and offer no further insight.

4 Conclusion

A multi-technique exploration of the impact of temperature cycling on CO_2 sorbents consisting of SCEI grafted onto silica substrates was undertaken to understand how repeated regeneration could affect CO_2 adsorption capacities under DAC-like CO_2 concentrations of 400 μLL^{-1}. For comparison, capacity measurements were also performed at much larger CO_2 concentrations of 50000 μLL^{-1} (5% by volume).

Samples were characterized with several methodologies: adsorption capacities at 400 $\mu L L^{-1}$ CO_2 were measured with a recently validated in-house DCB apparatus; TGA was used to determine amine/organic loadings, as well as adsorption capacities at high CO2 concentrations of 5%; FTIR was employed to monitor surface chemistry; and morphology was determined with SEM. Following an initial property analysis of the freshly synthesized sample, each substrate was subjected to numerous (up to 300) temperature cycles consisting of a 300 s ramp to 80 ◦C followed by a 300 s cooling ramp back to near room temperature. Temperature cycling was interrupted periodically to remove a small fraction of material and recharacterize the sample properties at that point in the thermal cycling process. Cycling of the remaining material was continued until the measured adsorption capacities at 400 $\mu L L^{-1}$ CO_2 approached zero.

The sorbents studied were synthesized in-house and consisted of diethyleneimine chains (DAS precursor) or triethyleneimine chains (TAS precursor) grafted onto two high-surface-area silica supports, MCM-41 and SBA-15. In particular, the present work focused on rapid thermal cycling of these easily-synthesized materials using CO_2-free air to differentiate the effects of repeated adsorptive exposure from thermal cycling in an oxidative environment alone. All sorbents were found to decrease in adsorption capacity after a large number of cycles; however, DAS-derived sorbents were in general more robust, maintaining a high capacity for a large number of cycles and more slowly deteriorating at higher cycle numbers. The TAS-derived sorbents were found to decrease in capacity after a much smaller number of cycles, which is likely due to cross linking of the secondary amines or imine formation possibly enhanced by repeated exposure to oxygen during the cold portions of the thermal cycles. In both DAS and TAS materials, the SBA-15 samples had higher capacities compared to the MCM-41 samples.

The behavior of the CO_2 adsorption capacity under thermal cycling was found to be different under DAC-like conditions of 400 $\mu L L^{-1}$ CO_2 in comparison to that observed at 50000 $\mu L L^{-1}$ CO_2. Except for the DAS/SBA-15 samples, which were robust under DAC conditions even up to 300 cycles, temperature cycling decreased the relative adsorption capacity markedly faster at a CO_2 concentration of 400 $\mu L L^{-1}$ than at 5%. We hypothesize that differences are due to the decreased mobility of the primary amines, which has been shown in previous theoretical work to be a significant factor in primary amine–CO_2 reactivity (and thus binding) in these systems. In addition, the MCM-41 samples both showed lower amine loading than the SBA-15 materials and are therefore expected to have concomitant lower densities (assuming approximate homogeneity across the surfaces), which would lead to a slower decrease overall in the low-concentration adsorption capacity. Better understanding would likely result by further probing the relationship between the variations in adsorption capacity and the surface density of the SCEI chains, including a robust chemical analysis.

Declarations

Conflicts of Interest:

All authors disclose no competing conflicts of interest. The full description of the procedures used in this paper is facilitated by identification of certain commercial products and their suppliers. The inclusion of such information should in no way be construed as indicating that such products or suppliers are endorsed or recommended by the authors or NIST or that they are necessarily the best materials, instruments, software or suppliers for the purposes described.

Author Contribution

C.M.W, W.S.M, M.D.M, and Z.T participated in data curation and formal analysis. C.M.W, W. S. M, and A.L.F. conceptualized, supervised, and wrote the manuscript. All authors contributed in the review of the manuscript.

Acknowledgement

Charlotte M. Wentz would like to gratefully acknowledge fundingthrough NIST Award # 70NANB8H165. Zois Tsinas wouldlike to gratefully acknowledge funding through NIST Award #70NANB22H140. This work was funded internally as part of theNIST Carbon Removal, Capture, Use, and Sequestration programdirected by Pamela M. Chu.

Data Availability

The data supporting this article have been included as part of theSupplementary Information.

References

1. Sanz-Perez, E.S., Murdock, C.R., Didas, S.A., Jones, C.W.: Chem. Rev. **116**, 11840–11876 (2016)
2. Lai, J.Y., Ngu, L.H., Hashim, S.S.: Greenh. Gases Sci. Technol. **11**, 1076–1117 (2021)
3. Dziejarski, B., Serafin, J., Anderson, K., Kry˙zy´nska, R.: Mater. Today Sustain. **24**, 100483 (2023)
4. Olajire, A.A.: Energy. **35**, 2610–2628 (2010)
5. Wilberforce, T., Olabi, A., Sayed, E.T., Elsaid, K., Abdelkareem, M.A.: Sci. Total Environ. **761**, 143203 (2021)
6. Goren, A.Y., Erdemir, D., Dincer, I.: Environ. Res. **240**, 117503 (2024)
7. McGivern, W.S., Nguyen, H.G.T., Manion, J.A.: Ind. Eng. Chem. Res. **62**, 8362–8372 (2023)
8. Fernandes, J.C., Brito, P., Travagin, F., Miletto, I., Giovenzana, G.B., Gianotti, E.: J. Phys. Chem. B. **126**, 7166–7171 (2022)
9. Heydari-Gorji, A., Belmabkhout, Y., Sayari, A.: Microporous Mesoporous Mater. **145**, 146–149 (2011)

10. Wentz, C.M., Tsinas, Z., Forster, A.L.: J. Visualized Experiments. **199**, e65845 (2023)
11. Anyanwu, J.-T., Wang, Y., Yang, R.T.: Chem. Eng. J. **427**, year (2022)
12. Carter, M., Nguyen, H.G.T., Allen, A.J., Yi, F., Yang, W.-C.D., Baumann, A.E., McGivern, W.S., Manion, J.A., Kuzmenko, I., Tsinas, Z., Wentz, C.M., Wenny, M., Siderius, D.W., van Zee, R.D., Stafford, C.M., Brown, C.M.: Journal CO2 Utilization. **89**, 102975 (2024)
13. Builes, S., Vega, L.F.: Langmuir. **29**, 199–206 (2013)
14. Hiyoshi, N., Yogo, K., Yashima, T.: Microporous Mesoporous Mater. **84**, 357–365 (2005)
15. Srikanth, C.S., Chuang, S.S.C.: ChemSusChem. **5**, 1435–1442 (2012)
16. Lashaki, M.J., Khiavi, S., Sayari, A.: Chem. Soc. Rev. **48**, 3320 (2019)
17. Sayari, A., Heydari-Gorji, A., Yang, Y.: J. Am. Chem. Soc. **134**, 13834–13842 (2012)
18. Bali, S., Chen, T.T., Chaikittisilp, W., Jones, C.W.: Energy Fuels. **27**, 1547–1554 (2013)
19. Ahmadalinezhad, A., Sayari, A.: Phys. Chem. Chem. Phys. **16**, 1529–1535 (2014)
20. Pang, S.H., Lee, L.-C., Sakwa-Novak, M.A., Lively, R.P.: J. Am. Chem. Soc. **139**, 3627–3630 (2017)
21. Li, S., Ceron, M.R., Eshelman, H.V., Varni, A.J., Maiti, A., Akhade, S., Pang, S.H.: ChemSusChem. **16**, e202201908 (2023)
22. Wang, D., Wang, X., Song, C.: ChemPhysChem. **18**, 3163–3173 (2017)

Figures

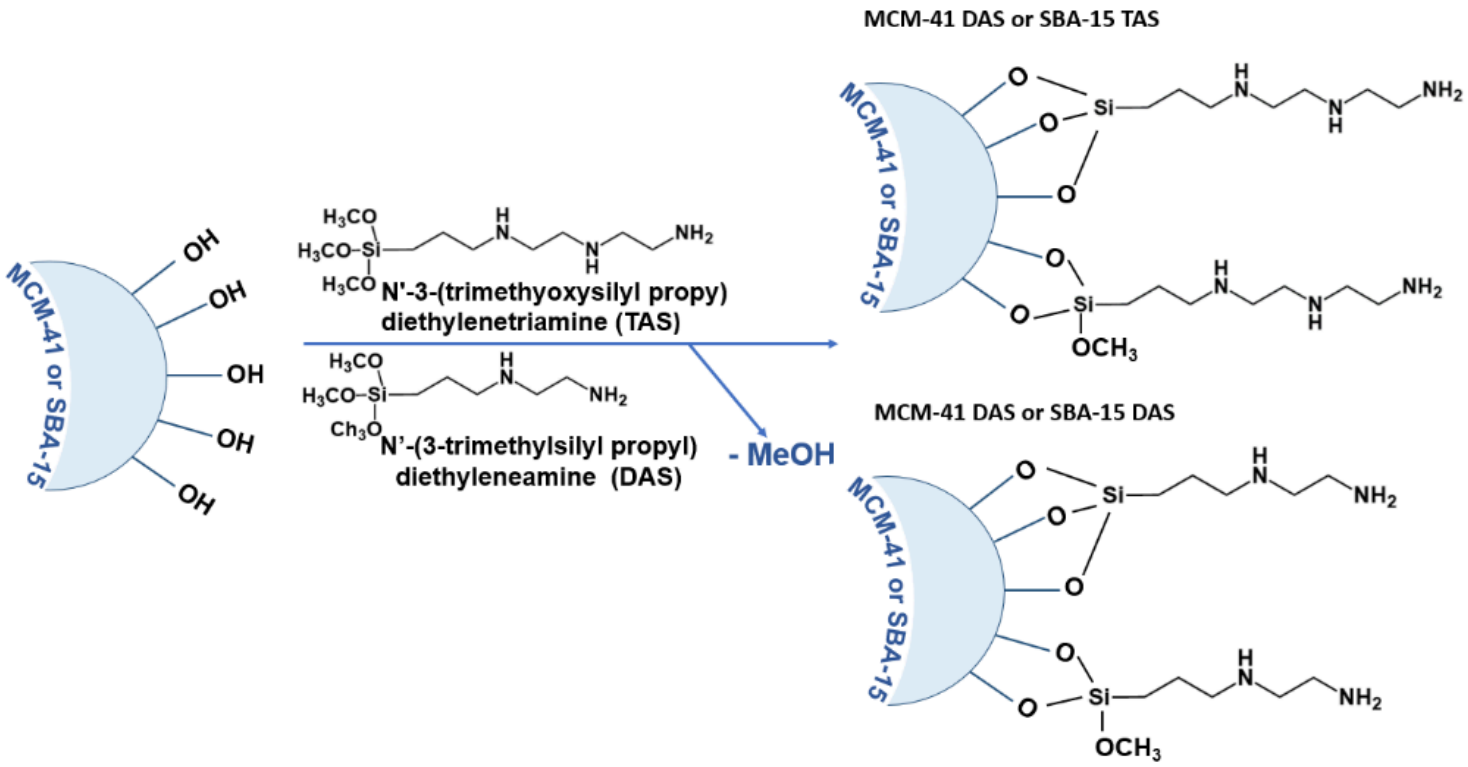


Figure 1

DAS or TAS grafted to silica substrate.

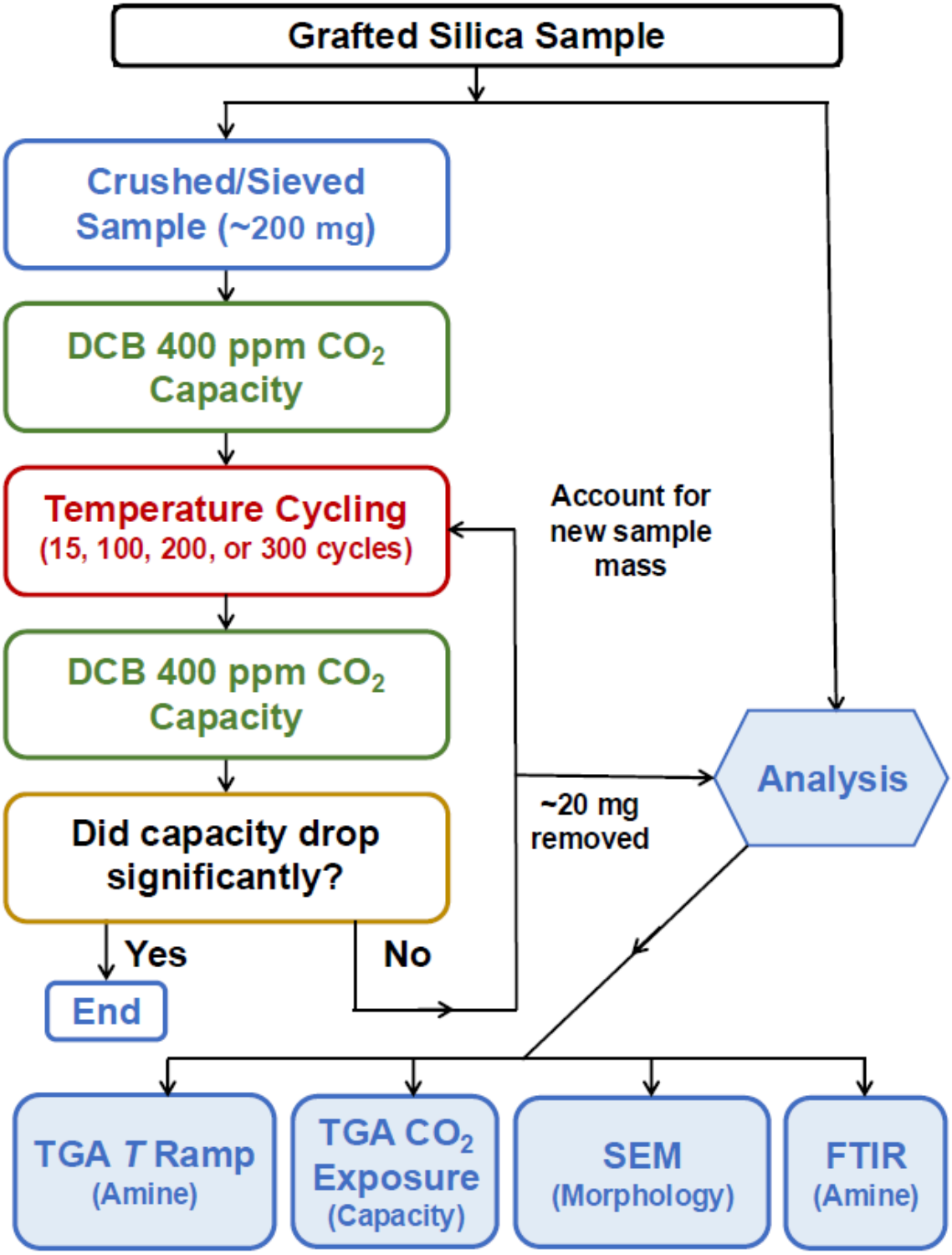


Figure 2

Diagram of analyses and sample aliquots

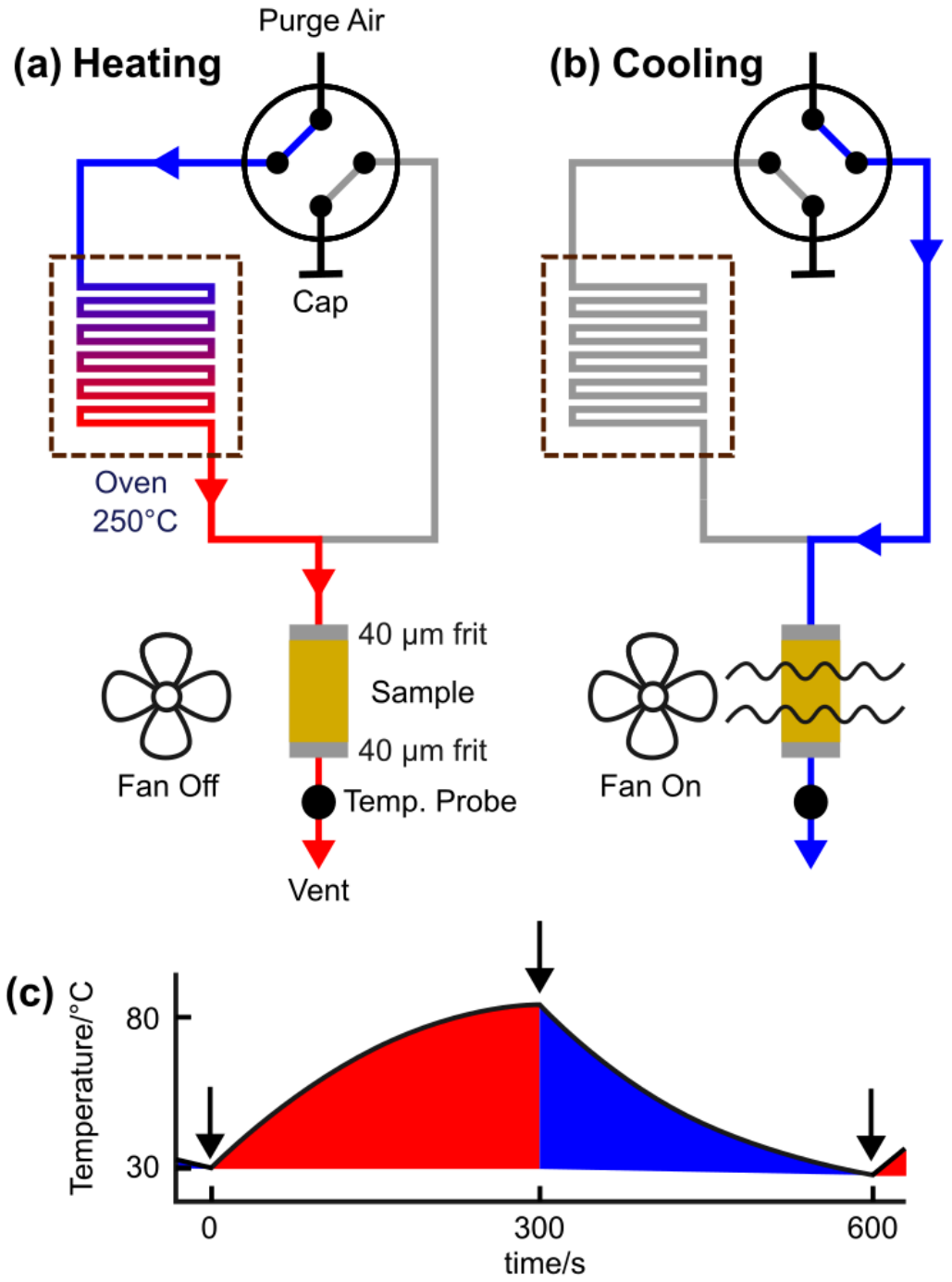


Figure 3

Schematic of temperature cycling apparatus and the corresponding column temperature profile. (a) Heating phase (300 s): a four-port, two-position rotary valve is oriented to flow purge air though an oven and then the sample; (b) Cooling phase (300 s): valve is oriented to direct room-temperature purge air through the sample with cooling actively aided by an external fan; (c) Schematic plot of the column temperature profile during a single cycle; the arrow at t = 0s indicates the valve rotation to start the

heating phase, the arrow at t = 300 s shows the switch to the cooling phase by a second valve rotation, and the arrow at t = 600s indicates a rotation to the initial orientation to start the next cycle.

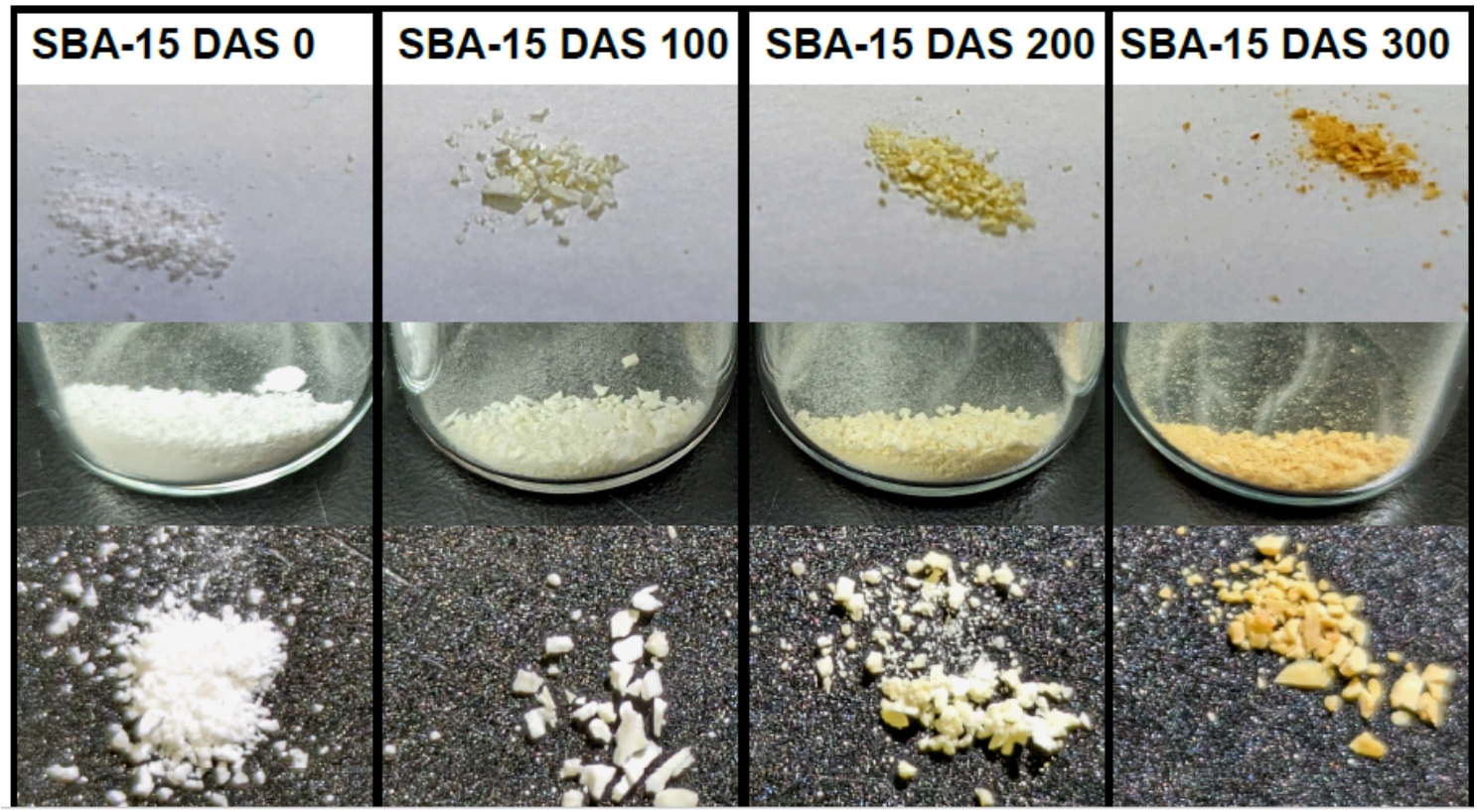


Figure 4

Images of DAS/SBA-15 material under lab lighting with a white background (top), in vials (middle), and with a black background (bottom). DAS/SBA-15 at 0 cycles (neat prior to formation of granules), 100 cycles, 200 cycles, and 300 cycles from left to right, respectively.

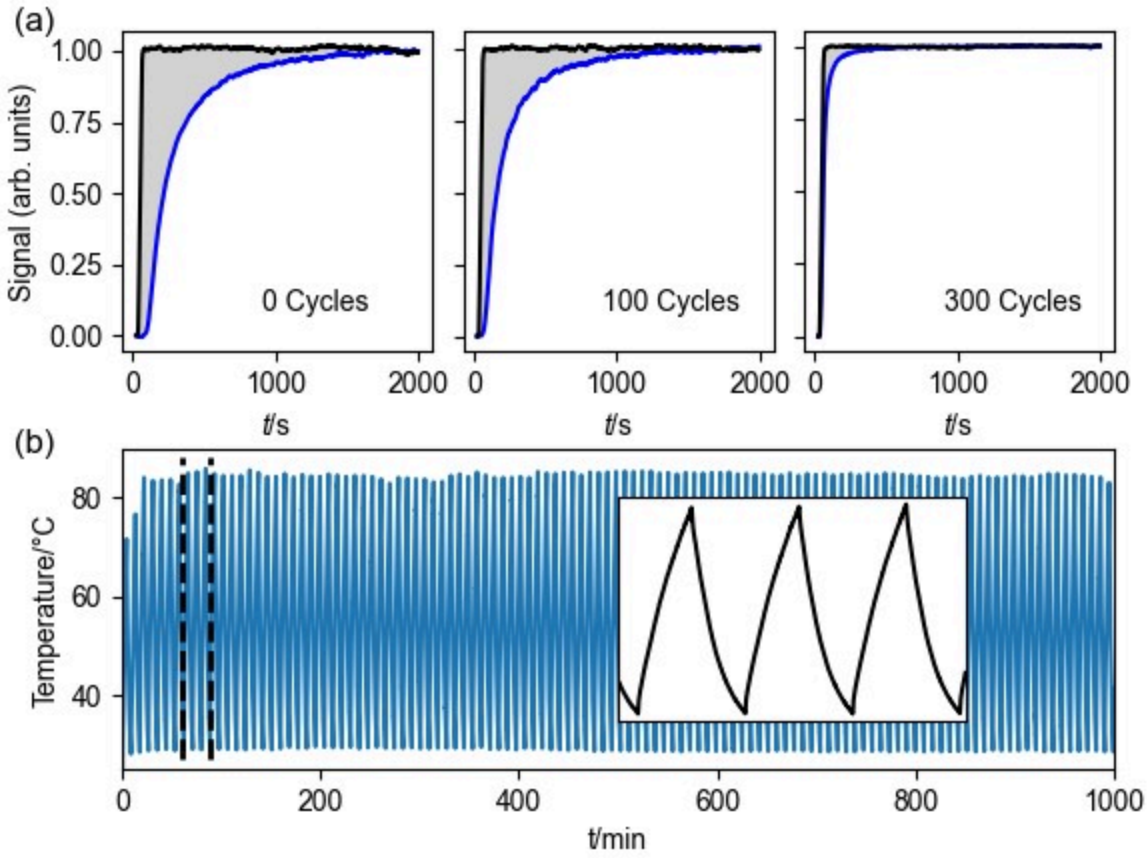


Figure 5

Dynamic column breakthrough instrument measurements at 0.6 hPa CO_2, 298.1K, and 1100 hPa pressure. Shown are the MS *m/z* 44 signals obtained for the sorbent column (blue solid curves) and the blank (black curves); (a) DAS/MCM-41 before thermal cycling, 0 cycles, (approximately ≈0.29 mmol CO_2/g), DAS/MCM-41 after thermal cycling 100 times (approximately 0.24 mmol CO_2/g, and DAS/MCM-41 after thermal cycling 300 times (approximately 0.03 mmol CO_2/gram); (b) Temperature profile of the thermal cycling for 100 oscillating temperature cycles between approximately 25 ◦C to 80 ◦C. The inset shows the individual temperature cycles indicated by the vertical dashed lines

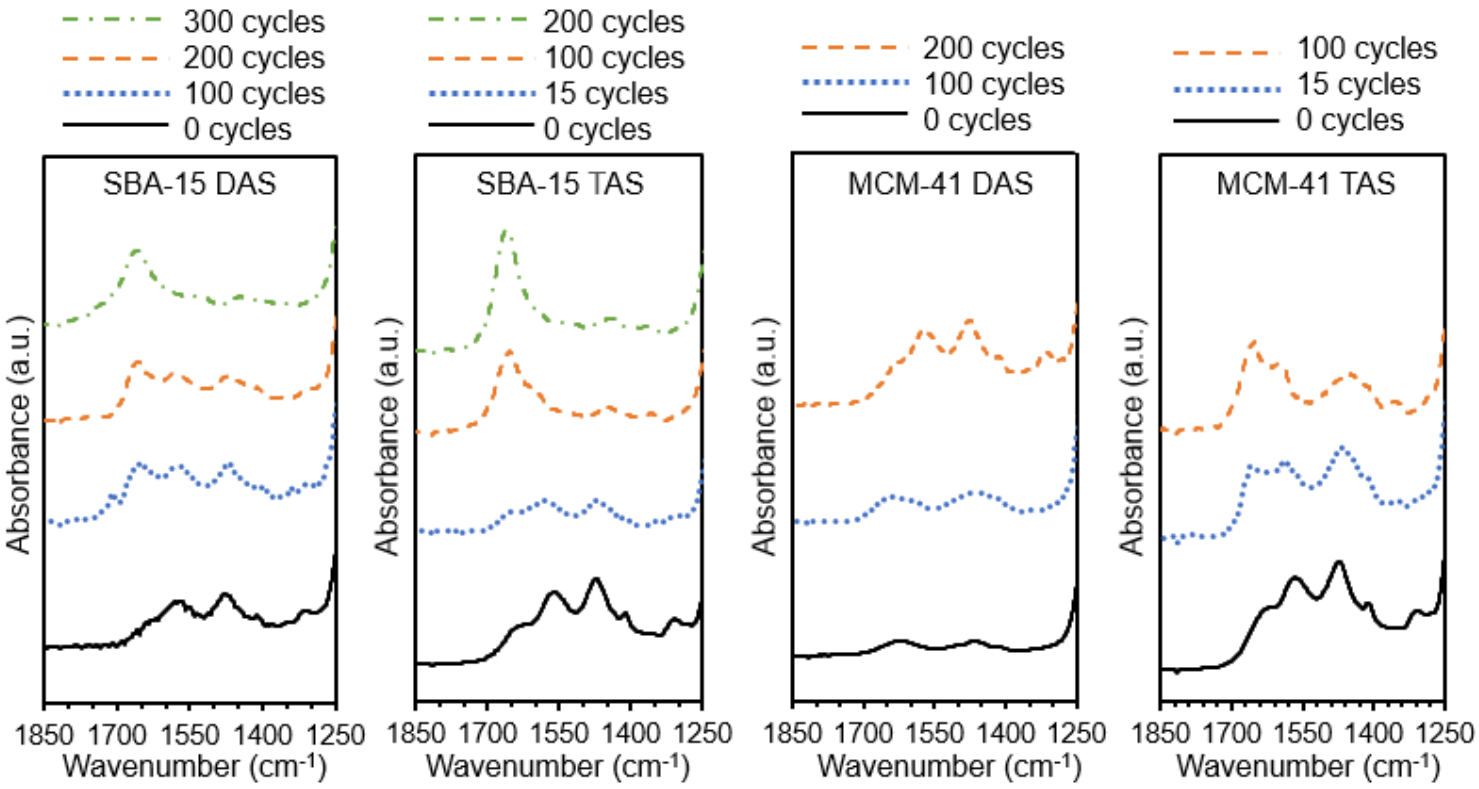


Figure 6

FTIR-ATR spectra of amine graphed silica composites through the thermal cycling procedure. To highlight the area of interest, only the region between 1850 cm^{-1} and 1250 cm^{-1} is displayed. The full spectra are provided as supporting information†.

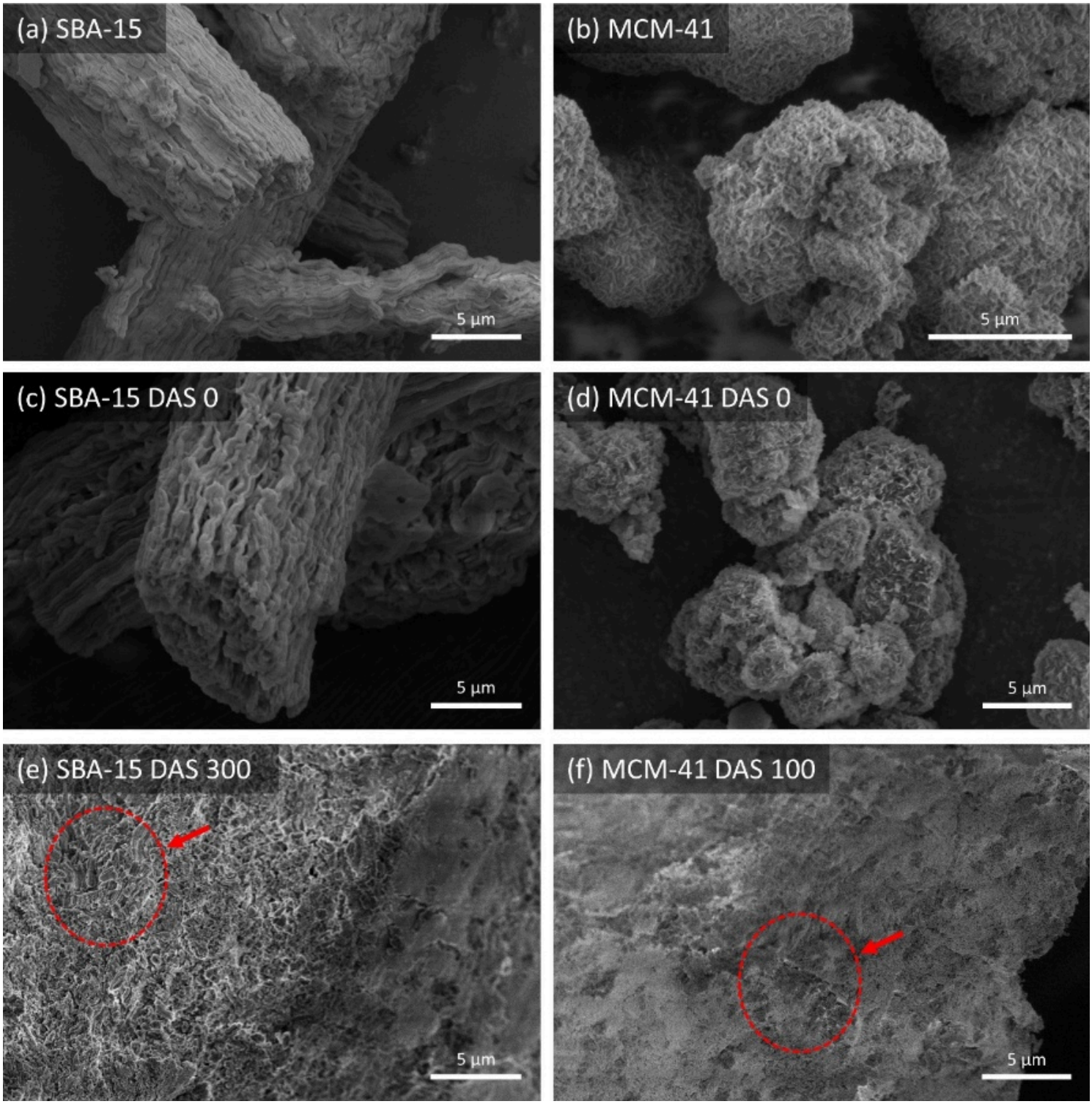


Figure 7

SEM micrographs of (a) neat SBA-15 and (b) neat MCM-41 substrates, as received; (c) DAS/SBA-15 and (d) DAS/MCM-41 at 0 cycles (prior to granule formation); (e) DAS/SBA-15 at 300 cycles and (f) DAS/MCM-41 at 100 cycles (granules).

Supplementary Files

This is a list of supplementary files associated with this preprint. Click to download.

- supp.pdf
- floatimage11.png